Emulating the paired-pulse facilitation of a biological synapse with a NiOx-based memristor

Hu, S. G.; Liu, Y.; Liu, Z.; Yu, Q.; Deng, L. J.; Yin, Y.; Chen, Tupei; Hosaka, Sumio

2013

Emulating the paired-pulse facilitation of a biological synapse with a NiOx-based memristor

S. G. Hu, Y. Liu, T. P. Chen, Z. Liu, Q. Yu, L. J. Deng, Y. Yin, and Sumio Hosaka
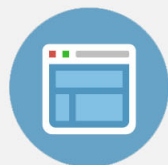
Emulating the paired-pulse facilitation of a biological synapse with a NiOx-based memristor

S. G. Hu,[1] Y. Liu,[1,a)] T. P. Chen,[2,b)] Z. Liu,[3] Q. Yu,[1] L. J. Deng,[1] Y. Yin,[4] and Sumio Hosaka[4]

[1]*State Key Laboratory of Electronic Thin Films and Integrated Devices, University of Electronic Science and Technology of China, Chengdu, People's Republic of China*
[2]*School of Electrical and Electronic Engineering, Nanyang Technological University, Singapore 639798*
[3]*School of Materials and Energy, Guangdong University of Technology, Guangzhou 510006, China*
[4]*Graduate School of Engineering, Gunma University, 1-5-1 Tenjin, Kiryu, Gunma 376-8515, Japan*

We study the paired-pulse-induced response of a NiOx-based memristor. The behavior of the memristor is surprisingly similar to the paired-pulse facilitation of a biological synapse. When the memristor is stimulated with a pair of electrical pulses, the current of the memristor induced by the second pulse is larger than that by the first pulse. In addition, the magnitude of the facilitation decreases with the pulse interval, while it increases with the pulse magnitude or pulse width. © 2013 AIP Publishing LLC. [http://dx.doi.org/10.1063/1.4804374]

In cognitive neuroscience, it is widely believed that changing the strength or weight of connections between neurons (i.e., synapses) is the mechanism for encoding and storing memory links in the nervous system.[1–3] Solid-state devices that use principles of biological synapses are essential for building cognitive computing systems and mimicking neural networks. Various techniques based on CMOS circuits have been used to implement synapses,[4–6] but such techniques are either inefficient or very complicated. Recently, the memristor has emerged as a promising candidate.[7–10] The resistance of a memristor depends on its past states, and this can be used to mimic the synaptic connections in a biological nervous system. Various synapse-like functions of memristors, such as synaptic plasticity,[11,12] spike-time-dependent plasticity,[13–16] and self-learning ability,[17–19] have been reported. A topical review on memristor-based neural networks was recently published by Thomas.[20]

Figure 1(a) shows a schematic of a biological synapse between a pre-synaptic neuron and a post-synaptic neuron. The synaptic strength is modified by the concentrations of the ionic species (e.g., Na^+, Ca^{2+}, Mg^{2+}) that activate or inhibit the release of neurotransmitters and receptors.[2] Synaptic enhancement, which is prominent on the timescale of tens to hundreds of milliseconds, is referred to as facilitation. With a pair of stimuli, the second post-synaptic current (or post-synaptic potential) can be up to several times larger than the magnitude of the first, as shown in Fig. 1(a). This effect is usually called paired-pulse facilitation (PPF).[2,3] In this work, we demonstrate that the response of a NiOx-based memristor to paired-pulse stimulation resembles the PPF of a biological synapse.

The synthesis of the memristor started with thermal growth of a 400 nm SiO_2 thin film on a p-type silicon wafer. After that, a 120 nm Ni layer was deposited on the SiO_2 film with electron-beam evaporation. A NiO thin film of ~150 nm was then deposited onto the Ni/SiO_2/Si substrate

by rf (13.6 MHz) magnetron sputtering of a NiO target (>99.99% purity). The rf power used here was 250 W. Finally, a 150 nm Au/15 nm Ni layer was deposited onto the NiO thin film by electron-beam evaporation to form the top electrode with a diameter of 200 μm. The chemical states of the synthesized nickel oxide thin film were analyzed with a Kratos AXIS x-ray photoelectron spectrometer equipped with monochromatic Al $K\alpha$ (1486.71 eV) x-ray radiation (12 kV and 15 mA). A Ni^0 peak is located within the Ni $2p$ band, indicating that the as-deposited nickel oxide thin film is Ni-rich. Paired-pulse generation and current measurement were conducted with a Keithley-4200 semiconductor characterization system at room temperature.

Figure 1(b) shows the currents of the memristor in response to a pair of voltage pulses. The situation is analogous to the PPF in a biological synapse illustrated in Fig. 1(a). As shown in Fig. 1(b)), a pair of pulses with a magnitude of 2 V, width of 5 ms, and interval of 10 ms was applied to the memristor; a current was produced in the device immediately following the pulses. Surprisingly, the current generated by the second pulse was 1.91 times larger than that by the first pulse, which is similar to the PPF behavior of a biological synapse (Fig. 1(a)).

The synaptic-PPF-like behavior of the memristor in Fig. 1(b) can be explained with the conductive filament model.[21,22] The metallic nickel phases in the Ni-rich oxide form conductive filaments in the oxide, allowing for ohmic conduction between the top and bottom electrodes of the device. During application of the first pulse, some Ni atoms in the oxide matrix migrate along the grain boundaries because of the applied electric field and local Joule heating caused by the extremely high local current density, forming additional local conductive filaments.[21,22] As such, after the first pulse, there are more local conductive filaments, and/or the original filaments have become bigger, leading to a decrease in the oxide resistance between the two electrodes. Therefore, the current of the second pulse is larger than that of the first.

The PPF of the memristor is defined with the equation[3]

$$PPF = 100\% \cdot (I - I_0)/I_0, \tag{1}$$

a)Email: yliu1975@uestc.edu.cn
b)Email: echentp@ntu.edu.sg
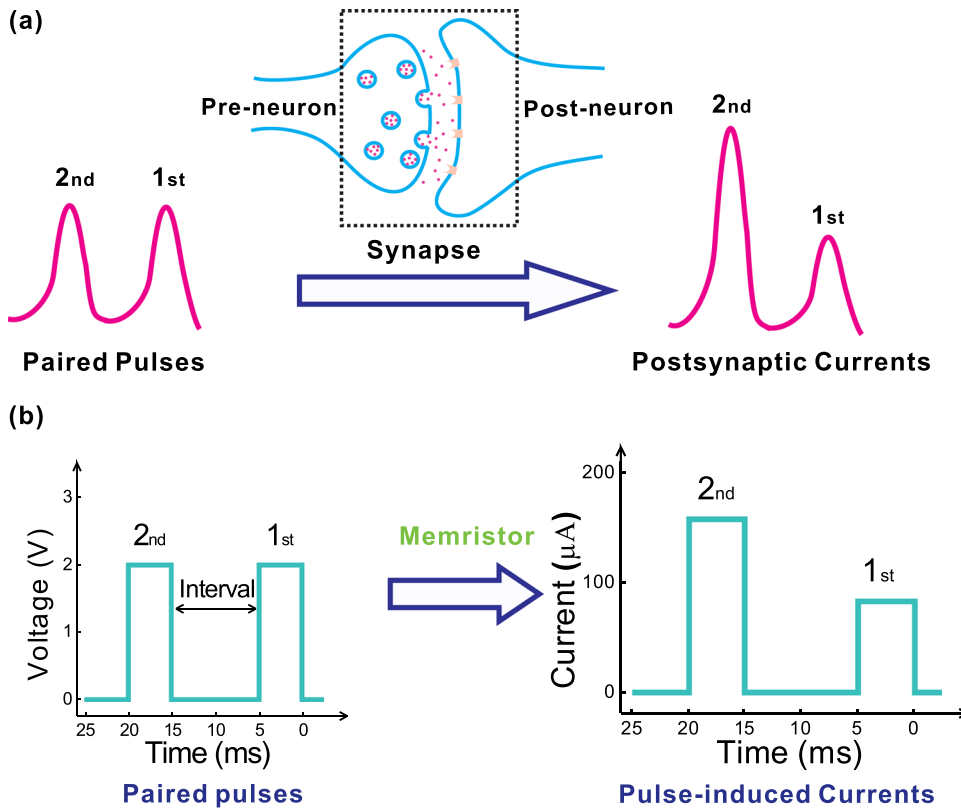
(a)

(b)

FIG. 1. (a) Schematic illustration of the PPF behavior of a biological synapse between a pre-synaptic neuron and a post-synaptic neuron.[2] The synaptic strength is modified by the concentrations of the ionic species (e.g., Na^+, Ca^{2+}, Mg^{2+}). With a pair of stimuli, the post-synaptic current (or post-synaptic potential) induced by the second pulse is larger than that by the first pulse. (b) The PPF phenomenon of a NiO_x-based memristor observed in the present study. A pair of voltage pulses were applied to the memristor (the left panel), and the corresponding current of the memristor was measured (the right panel).

where I_0 and I are the currents of the first and second pulses, respectively. Figure 2 shows the PPF as a function of the interval between the paired pulses. Here, the pulse magnitude and width were fixed at 1.8 V and 5 ms, respectively. The pulse interval was varied from 5 ms to 2000 ms. The currents I_0 and I were measured during the first and second pulses, respectively. For each pulse interval, at least 10 devices at different locations on the wafer were examined, and the statistical distribution of the PPF for each pulse interval is shown in Fig. 2. Note that all the PPF measurements in
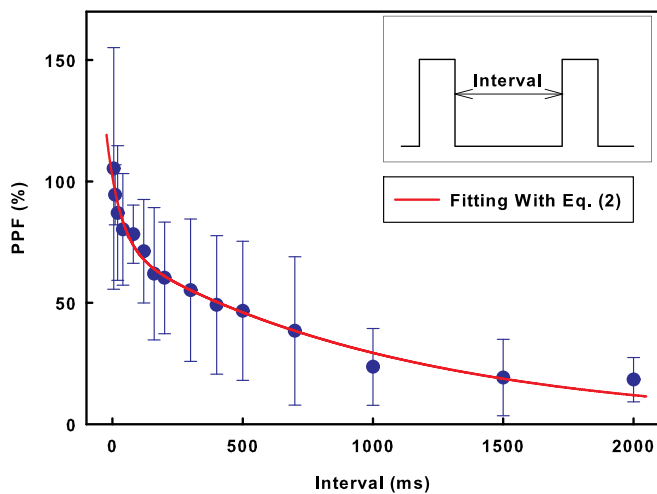

FIG. 2. PPF of the memristor as a function of the pulse interval with the pulse magnitude and width fixed at 1.8 V and 5 ms, respectively. The PPF measurement was conducted on 10 virgin devices for each pulse interval. The inset illustrates the pattern of a pair of voltage pulses with a pulse interval between the two pulses applied to the memristor. The fitting with Eq. (2) to the measured PPF values yields $c_1 = 30\%$, $c_2 = 72\%$, $\tau_1 = 53$ ms, and $\tau_2 = 1111$ ms.

this work were conducted on virgin devices. As can be observed in the figure, the PPF is positive for all the pulse intervals, showing that the current of the second pulse is always larger than that of the first. This indicates that the effect of the first pulse prolonged the period of the second pulse. However, the PPF decreases gradually with the pulse interval. The average PPF is 105.4% for the interval of 5 ms and decreases to 18.3% for the interval of 2000 ms. This means that the effect of the first pulse faded away gradually during the pulse interval, which suggests that the oxide that had undergone the changes caused by the first pulse could return to its original state if the pulse interval was very long.

The dependence of the PPF of the memristor on the pulse magnitude/pulse width was measured. For each measurement, at least 10 devices at different locations on the wafer were examined. Figure 3(a) shows the PPF as a function of the pulse magnitude with the pulse width and pulse interval fixed at 5 ms and 100 ms, respectively. As can be seen in the figure, the average PPF increases from 7% to 195% when the pulse magnitude increases from 1 V to 3 V. Figure 3(b) shows the PPF as a function of the pulse width with the pulse magnitude and pulse interval fixed at 2 V and 100 ms, respectively. The average PPF increases from 32% for the pulse width of 5 ms to 224% for the pulse width of 1000 ms. The results shown in Fig. 3 can be explained as follows. With a higher pulse voltage or longer pulse duration, more electrical energy was injected into the oxide during the first pulse, causing more local conductive filaments to form and/or the existing filaments to become bigger. This led to a lower oxide resistance, and therefore the current enhancement was larger.

In a biological synapse, PPF decay with pulse interval can be divided into a rapid phase lasting tens of milliseconds (F1) and a slower phase lasting hundreds of milliseconds
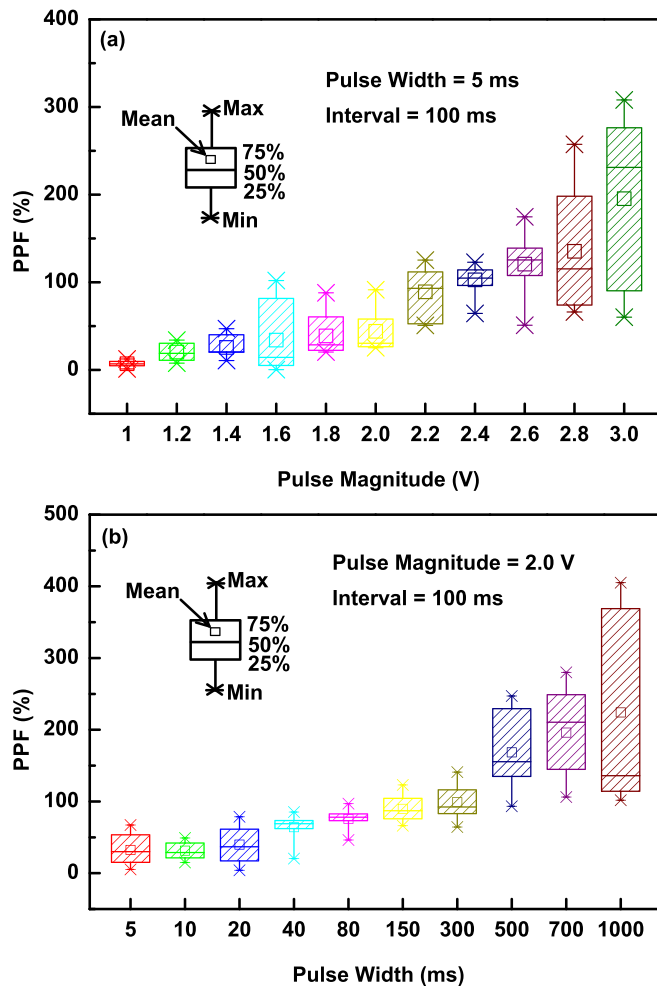
FIG. 3. PPF as a function of the pulse magnitude (a) and pulse width (b). A PPF measurement was conducted on 10 virgin devices, and the statistical distribution of the PPF value is shown in the figure. In (a), the pulse width and pulse interval were 5 ms and 100 ms, respectively; and in (b), the pulse magnitude and pulse interval were 2 V and 100 ms, respectively.

(F2).[2] Interestingly, as can be observed in Fig. 2, the dependence of the PPF of the memristor on the pulse interval also shows two-phase behavior, which can be described with the equation[2]

$$PPF = c_1 \cdot \exp(-t/\tau_1) + c_2 \cdot \exp(-t/\tau_2), \qquad (2)$$

where t is the pulse-off time (i.e., the pulse interval), c_1 and c_2 are the initial facilitation magnitudes of the respective phases, and τ_1 and τ_2 are the characteristic relaxation times of the respective phases. The physics for the two phases is not clear yet. In this work, Eq. (2) was used to fit the measured pulse-interval dependence of the PPF. In the fitting, τ_1 should be set smaller than τ_2 because τ_1 and τ_2 represent the rapid and slow phases, respectively;[2] however, all the parameters in Eq. (2) are independent variables. The fitting shown in Fig. 2 yields $c_1 = 30\%$, $c_2 = 72\%$, $\tau_1 = 53$ ms, and $\tau_2 = 1111$ ms. The time scales of the rapid and slow phases of the memristor are similar to those of a biological synapse.[2]

Figure 4 shows the effect of the pulse width/magnitude on the F1 and F2 facilitations. In this experiment, at least 10 devices at different locations on the wafer were examined for each pulse width or magnitude, and c_1, τ_1, c_2, and τ_2 were obtained by fitting Eq. (2) to the measured PPF data for each magnitude or width. As shown in Figs. 4(a) and 4(c), both c_1 and c_2 increase with the pulse magnitude or pulse width, indicating that both F1 and F2 facilitations are enhanced with a higher pulse voltage or longer pulse duration. On the other hand, as can be observed in Figs. 4(b) and 4(d), the characteristic relaxation times (τ_1 and τ_2) do not show a clear trend with the pulse magnitude or pulse width.

In conclusion, we have demonstrated that a NiO_x-based memristor can emulate the PPF of a biological synapse. The PPF of the memristor increases with both the pulse magnitude and pulse width. Being similar to the behavior of a biological synapse, the PPF decay of the memristor with pulse-off time can be divided into a rapid phase lasting tens
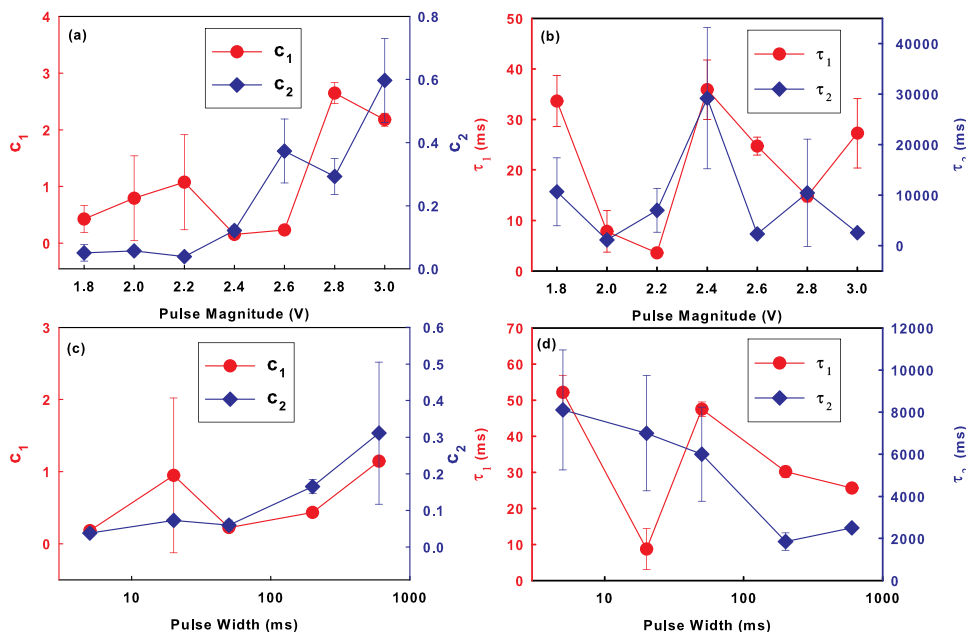

FIG. 4. Influence of the pulse magnitude and pulse width on the parameters c_1, c_2, τ_1, and τ_2. The values of the parameters were obtained from the fitting with Eq. (2) to the measured PPF values. A PPF measurement was conducted on 10 virgin devices.

of milliseconds and a slower phase lasting hundreds of milliseconds.

[1]S. Martin, P. Grimwood, and R. Morris, Annu. Rev. Neurosci. **23**, 649 (2000).

[2]R. S. Zucker and W. G. Regehr, Annu. Rev. Physiol. **64**, 355 (2002).

[3]P. P. Atluri and W. G. Regehr, J. Neurosci. **16**, 5661 (1996).

[4]J. M. Cruz-Albrecht, M. W. Yung, and N. Srinivasa, IEEE Trans. Biomed. Circuits Syst. **6**, 246 (2012).

[5]G. Indiveri, E. Chicca, and R. Douglas, IEEE Trans. Neural Netw. **17**, 211 (2006).

[6]K. D. Cantley, A. Subramaniam, H. J. Stiegler, R. A. Chapman, and E. M. Vogel, IEEE Trans. Neural Netw. Learn. Syst. **23**, 565 (2012).

[7]T. Tsuruoka, T. Hasegawa, K. Terabel, and M. Aono, Nanotechnology **23**, 435705 (2012).

[8]Z. Q. Wang, H. Y. Xu, X. H. Li, H. Yu, Y. C. Liu, and X. J. Zhu, Adv. Funct. Mater. **22**, 2759 (2012).

[9]S. G. Hu, H. T. Wu, Y. Liu, T. P. Chen, Z. Liu, Q. Yu, Y. Yin, and S. Hosaka, J. Appl. Phys. **113**, 114502 (2013).

[10]A. Nayak, T. Ohno, T. Tsuruoka, K. Terabe, T. Hasegawa, J. K. Gimzewski, and M. Aono, Adv. Funct. Mater. **22**, 3606 (2012).

[11]T. Ohno, T. Hasegawa, T. Tsuruoka, K. Terabe, J. K. Gimzewski, and M. Aono, Nature Mater. **10**, 591 (2011).

[12]S. Yu, Y. Wu, R. Jeyasingh, D. Kuzum, and H. S. P. Wong, IEEE Trans. Electron Devices **58**, 2729 (2011).

[13]S. J. Choi, G. B. Kim, K. Lee, K. H. Kim, W. Y. Yang, S. Cho, H. J. Bae, D. S. Seo, S. I. Kim, and K. J. Lee, Appl. Phys. A **102**, 1019 (2011).

[14]S. H. Jo, T. Chang, I. Ebong, B. B. Bhadviya, P. Mazumder, and W. Lu, Nano Lett. **10**, 1297 (2010).

[15]D. Kuzum, R. G. D. Jeyasingh, B. Lee, and H. S. P. Wong, Nano Lett. **12**, 2179 (2012).

[16]M. Ziegler, R. Soni, T. Patelczyk, M. Ignatov, T. Bartsch, P. Meuffels, and H. Kohlstedt, Adv. Funct. Mater. **22**, 2744 (2012).

[17]Y. Liu, T. P. Chen, Z. Liu, Y. F. Yu, P. Li, and S. Fung, Appl. Phys. A **105**, 855 (2011).

[18]T. Hasegawa, T. Ohno, K. Terabe, T. Tsuruoka, T. Nakayama, J. K. Gimzewski, and M. Aono, Adv. Mater. **22**, 1831 (2010).

[19]T. Chang, S. H. Jo, and W. Lu, ACS Nano **5**, 7669 (2011).

[20]A. Thomas, J. Phys. D: Appl. Phys. **46**, 093001 (2013).

[21]M. J. Lee, S. Han, S. H. Jeon, B. H. Park, B. S. Kang, S. E. Ahn, K. H. Kim, C. B. Lee, C. J. Kim, and I. K. Yoo, Nano Lett. **9**, 1476 (2009).

[22]S. G. Hu, Y. Liu, T. Chen, Z. Liu, M. Yang, Q. Yu, and S. Fung, IEEE Trans. Electron Devices **59**, 1558 (2012).